


Low-level laser therapy enhances the number of osteocytes in calvaria bone defects of ovariectomized rats

Priscilla Hakime Scalize¹ | Luiz Gustavo de Sousa¹ | Lígia Maria Napolitano Gonçalves¹ |
 Dimitrius Leonardo Pitol¹ | Marcelo Palinkas¹ | Antônio Augusto Coppi² |
 Mariah Acioli Righeti¹ | Vitória Ricardo¹ | Karina Fittipaldi Bombonato-Prado¹ |
 Simone Cecílio Hallak Regalo¹ | Selma Siessere¹ 

¹Department of Morphology, Physiology and Basic Pathology, School of Dentistry of Ribeirão Preto, USP - University of São Paulo, Ribeirão Preto, SP, Brazil

²Faculty of Health and Medical Sciences, School of Veterinary Medicine, University of Surrey, Guildford, Surrey, UK

Correspondence

Selma Siessere, Department of Morphology, Physiology and Basic Pathology, School of Dentistry of Ribeirão Preto, USP - University of São Paulo, Ribeirão Preto, SP, Brazil.
 Email: selmas@forp.usp.br

Funding information

FAPESP (São Paulo Research Foundation), Grant/Award Number: 2011/50686-0; National Institute and Technology - Translational Medicine (INCT.TM); CNPq (National Council for Scientific and Technological Development)

Abstract

Background: Osteoporosis can make bone repair difficult. Low-level laser therapy (LLLT) has been shown to be a promising tool for bone neoformation. This study aimed to analyze the effect of LLLT on calvaria bone defects of ovariectomized rats using stereology.

Methods: Fifty-four Wistar rats were subjected to bilateral ovariectomy, and bone defects were created in calvaria after 150 days. The animals were divided into nine groups (n = 6 per group), and 24 hours after the bone defects were created they received three, six or 12 sessions of LLLT at 0, 20 or 30 J/cm², using a 780-nm low-intensity GaAlAs laser. One-way ANOVA followed by Tukey's post hoc test was used for data processing. A difference of $P < 0.05$ was considered statistically significant. The parameters evaluated were osteocyte density (Nv_{ost}), total osteocyte number (Nto_{ost}), trabecular surface density (Sv_t), and trabecular surface area (Sa_t).

Results: Data obtained showed that Nto_{ost} , Sv_t , and Sa_t in group G2 rats were significantly different from G1 (0 J/cm²) ($P < 0.05$). Compared to group G4, G5 presented higher values for the parameters Sv_t and Sa_t , and G6 presented significantly higher values for almost all the analyzed parameters (Nv_{ost} , Nto_{ost} , Sv_t , and Sa_t) ($P < 0.05$). Compared to group G7, G8 showed a higher value only for the parameter Sa_t , and G9 showed significantly higher values for parameters Nv_{ost} , Nto_{ost} , Sv_t , and Sa_t .

Conclusion: We conclude that LLLT stimulated bone neoformation and contributed to an increase in the total number of osteocytes, especially with a laser energy density of 30 J/cm² given for six and 12 sessions.

KEYWORDS

bone, low-level laser therapy, osteocytes, osteoporosis

This is an open access article under the terms of the Creative Commons Attribution-NonCommercial License, which permits use, distribution and reproduction in any medium, provided the original work is properly cited and is not used for commercial purposes.

© 2019 The Authors. *Animal Models and Experimental Medicine* published by John Wiley & Sons Australia, Ltd on behalf of The Chinese Association for Laboratory Animal Sciences

1 | INTRODUCTION

The human skeleton is constantly remodeling, with the osteoclasts promoting the resorption of mature bone tissue and new matrix being formed by osteoblasts, allowing a balance between resorption and bone deposition. An imbalance in this process may cause osteoporosis,¹ a disease characterized by bone loss and deterioration of its microarchitecture, leading to bone fragility and fractures.²

There are several factors that may initiate osteoporosis: (a) estrogen deficiency in postmenopausal women; (b) alcohol consumption and cigarette smoking, which inhibit osteoblast proliferation and differentiation; (c) high caffeine intake, which leads to urinary calcium release; (d) an inadequate dietary routine, with an excess of fiber, protein, and sodium, which impairs calcium absorption; (e) and lack of physical exercise.² In recent years, osteoporosis has been treated as a public concern, because of longer life expectancy and the steady aging of the world population.³ Osteoporosis represents a challenge as much for doctors as for public finances. Because this disease brings high costs to individuals and society, the majority of people remain without adequate treatment. The main consequences for untreated osteoporosis are bone fractures, which may cause acute pain and loss of function, and require hospitalization or specialized home care.⁴ Thus, there is the need for strategies that prevent this degenerative disease and allow bone repair after disease onset.

Reports in the literature have demonstrated the potential of low-level laser therapy (LLLT) in bone tissue regeneration.⁵⁻¹⁰ Recently, our research group observed in an animal model of ovariectomy, which simulates the postmenopausal state in human females,¹¹ that rats receiving LLLT at 20 J/cm² over three sessions and 30 J/cm² over six and 12 sessions presented an increase in bone volume compared to control groups. Moreover, an increase in bone volume, measured using stereological parameters, was detected for the animals that received a laser fluence of 30 J/cm².⁹ These data led our group to evaluate in more depth the effects of laser treatment on bone metabolism, with the goal of analyzing the effects of 20 and 30 J/cm² fluences (over three, six, and 12 sessions) in bone tissue and its cells during the early stages of bone repair, using stereological parameters.

2 | METHODS

2.1 | Laser equipment

The equipment used for this study was a gallium-aluminum-arsenide (GaAlAs) semiconductor diode device Twin Laser (MM Optics, São Carlos, SP, Brazil). The main specifications for this equipment were: frequency of 50 Hz, input voltage of 100-240 V, power output of 70 mW, maximal dosage of 315 J/cm², and wavelength of 780 nm.

2.2 | Animals

Fifty-four Wistar rats (mean weight of 300 g) from the Central Campus of the USP of Ribeirão Preto vivarium were used in this study. The animals were maintained in polyethylene boxes, with

three rats per box, a daily temperature range of 23-24°C and a 12-hours light/dark cycle. All animals received food and water ad libitum.

2.3 | Ethical approval

All procedures performed involving the animals were in accordance with the ethical standards of the institution at which the studies were conducted (Ethics Committee for Animal Experimentation of the University of São Paulo, permit number 11.1.639.53.5). All applicable international, national, and/or institutional guidelines for the care and use of animals were followed.

2.4 | Ovariectomy surgery

The animals were weighed and anesthetized by an intramuscular injection of xylazine (10 mg/kg) and ketamine (75 mg/kg) (Agibrands do Brasil LTDA, Campinas, SP, Brazil). After trichotomy and antiseptis, the ovaries were excised. The tissue suture was performed with silk thread 4.0 (Ethicon, Johnson & Johnson, São José dos Campos, SP, Brazil). Each animal received an intramuscular injection of 0.1 mL/100 g weight of small-size veterinary pentabiotic (Fort Dodge[®], Campinas, SP, Brazil), followed by 0.2 mL/100 g of Banamine[®] injectable analgesic (Schering-Plough, Cotia, SP, Brazil). The success of the ovariectomy was evaluated by analyzing the estrous cycle 2 weeks after the surgical procedure¹² and the atrophy of uterine horns observed following the euthanasia of the animals.¹³

2.5 | Bone defect procedure

Bone defects were created 150 days after ovariectomy. Following the same surgery protocols, the animals were weighed and anesthetized by intramuscular injection of xylazine (10 mg/kg) and ketamine (75 mg/kg) (Agibrands do Brasil LTDA). The bone defect (5 mm wide, 1 mm deep) was created in the left portion of the parietal bone, using a trephine drill (Neodent, Curitiba, PR, Brazil) adapted to a counter-angle head with the aid of an electric implant motor (Dentscler, Ribeirão Preto, SP, Brazil) adjusted to 3000 rpm. Throughout the surgery, the trephine drill did not touch dura mater in order to maintain its integrity. All procedures were performed with 0.9 sterile saline solution and tissues were sutured with 4-0 silk suture (Ethicon, Johnson & Johnson, São José dos Campos, SP, Brazil). After the procedure, each animal received an intramuscular injection of 0.1 mL/100 g weight of small-size veterinary pentabiotic (Fort Dodge[®], Campinas, SP, Brazil). The animals were divided in nine groups (n = 6 per group).

2.6 | Laser application

The following treatments were applied to the groups, as described in Table 1.

For each session the animals were sedated in accordance with the previously described protocol. Equipment calibration was

performed before the sessions. The animals received laser treatment from the day after the last surgery until sacrifice at 48-hour intervals. The laser was applied at five different sites (four peripheral [3, 6, 9, and 12 hours clock position] and one central to the defect). Groups 1, 4, and 7 represent control animals that received a simulated laser application (0 J/cm²) over three, six, and 12 sessions, respectively. The same sedation protocol and laser specifications (40 mW potency, 780 nm wavelength, and 1.0 W/cm² irradiance, continuous mode, perpendicular beam and contact application) were used in all the groups. For the 20 J/cm² applications, in each session, total irradiation time was 100 seconds, application time per site was 20 seconds and released energy was 4.0 J. For the 30 J/cm² applications, in each session, total irradiation time was 150 seconds, application time per site was 30 seconds and released energy was 6.0 J. The rats were sacrificed to remove calvaria samples 24 hours after the last laser session, at 7 (groups 1-3), 13 (groups 4-6), and 25 days (groups 7-9) after defect creation.

2.7 | Histological processing

After fixation (4% formaldehyde for 24 hours) and decalcification (0.5 M EDTA + TRIS for 30 days), the fragments were dehydrated by gradual exposure to ethanol (70% for 2 hours and 90% for 2 hours), then infiltrated by 95% alcohol and historesin for 3 hours, and finally embedded in pure historesin for over 3 hours. Isotropic uniformly-random (IUR) 2.5 μm sections (using a Leica RM 2255 microtome, Germany) were obtained using the isector method¹⁴ and sampled using the Smooth Fractionator principle.¹⁵ Ten slides per animal were obtained, representing the whole area of bone defect. Sections were subsequently stained with hematoxylin and eosin. Digital images were obtained with a DFC 310 FX camera (Leica, Wetzlar, Germany) coupled with a DM 4000B light microscope (Leica).

2.8 | Design-based stereology

The following quantities were estimated: osteocyte numerical density ($N_{v_{ost}}$), total osteocyte number (N_{ost}), trabecular surface density

TABLE 1 Experimental groups

Groups	Treatments (J/cm ²)		
	Three sessions	Six sessions	12 sessions
1	0 (control)		
2	20		
3	30		
4	0		
5	20		
6	30		
7			0
8			20
9			30

(Sv_t), and trabecular surface area (Sa_t). To calculate N_{ost} and Sa_t parameters the values of V_{tr} (total volume of repaired tissue) formerly evaluated by our research group were used.⁹

In order to estimate the osteocyte numerical density, the two-way physical disector method was employed,¹⁶ using the following formula:

$$N_{v_{ost}} = \sum Q^- / a(f) \times h \quad (1)$$

where $\sum Q^-$ is the total number of osteocyte nuclei sampled using dissectors, $a(f)$ is the area of each frame used to sample osteocytes nuclei, and h is the disector height.

The total number of osteocytes (N_{ost}) was then obtained using the following formula:

$$N_{ost} = N_{v_{ost}} \times V_{tr} \quad (2)$$

where $N_{v_{ost}}$ is the osteocyte numerical density and V_{tr} the total volume of the repaired tissue.

To estimate the trabecular surface area (Sa_t) it was necessary to estimate the trabecular surface density (Sv_t) first by employing the following formula:

$$Sv_t = 2 \sum I / \ell \sum Pe \quad (3)$$

where $\sum I$ is the total number of intersections with the trabeculae, ℓ the length of the test-line and $\sum Pe$ the total number of test-points hitting the repaired tissue.

To estimate the trabecular surface area (Sa_t), the following formula was used:

$$Sa_t = Sv_t \times V_{tr} \quad (4)$$

where Sv_t is the trabecular surface density and V_{tr} is the total volume of the repaired tissue.

For the estimations conducted here, ie, total volume of the repaired tissue and trabecular surface area, no correction for global shrinkage was applied since inter-group differences were not statistically significant.

2.9 | Statistical analysis

The quantitative data were analyzed using spss version 21.0 for Windows (SPSS Inc., Chicago, IL, USA). ANOVA followed by Tukey's post hoc test was used for data processing. A difference of $P < 0.05$ was considered statistically significant.

3 | RESULTS

All animals were in diestrus phase, with a predominance of leucocytes in vaginal fluid observed under a light microscope, and thin and atrophic uterine horns.

The histological images show that the groups that received LLLT at 20 and 30 J/cm² for three sessions presented new bone formation at the periphery of the defect, but a greater amount of newly formed bone was evident in the group receiving 20 J/cm². On the other hand, in the control group receiving 0 J/cm² for three sessions,

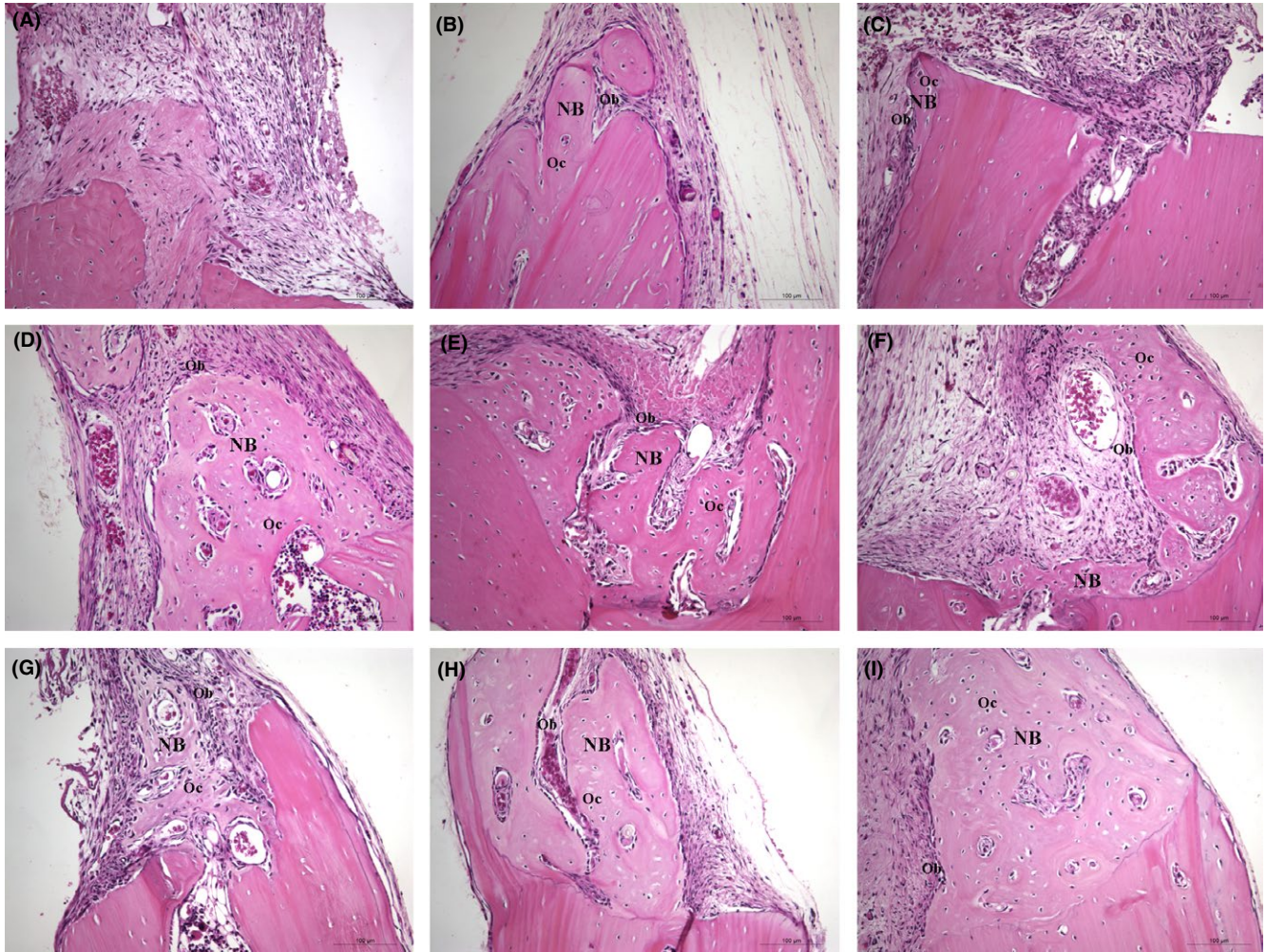


FIGURE 1 Photomicrographs of bone defect periphery region. A, G1 (three sessions; 0 J/cm²); B, G2 (three sessions; 20 J/cm²); C, G3 (three sessions; 30 J/cm²); D, G4 (six sessions; 0 J/cm²); E, G5 (six sessions; 20 J/cm²); F, G6 (six sessions; 30 J/cm²); G, G7 (12 sessions; 0 J/cm²); H, G8 (12 sessions; 20 J/cm²); I, G9 (12 sessions; 30 J/cm²). NB, newly formed bone; Ob, osteoblasts; Oc, osteocytes. Hematoxylin and eosin stain; Scale bar, 100 μ m

organized connective tissue in the periphery of the bone defect was observed. In all groups treated for six sessions, it was possible to observe bone neof ormation in the periphery of the defect with osteocytes in lacunae and osteoblasts adjacent to the neof ormed trabeculae. The same was observed in the groups treated for 12 sessions (Figure 1).

Tables 2-4 show the estimated stereological parameters for the groups receiving, respectively, three, six, and 12 LLLT sessions. In the groups that received three LLLT sessions (G1, G2, and G3), it was observed that for the parameters N_{ost} , Sv_t , and Sa_t , group G2 (20 J/cm²) presented significantly higher values compared to G1 (0 J/cm²; $P < 0.05$).

In the groups that received six LLLT sessions (G4, G5, and G6), it was observed that G5 (20 J/cm²) presented significantly higher values for parameters Sv_t and Sa_t , compared to G4 (0 J/cm²; $P < 0.05$). On the other hand, G6 (30 J/cm²) presented significantly higher values for almost all the analyzed parameters (Nv_{ost} , N_{ost} , Sv_t , and Sa_t) compared to G1 (0 J/cm²; $P < 0.05$).

Considering the results obtained in the groups that received 12 sessions of LLLT (G7, G8, and G9), G8 (20 J/cm²) showed a higher value than G7 (0 J/cm²) only for parameter Sa_t ($P < 0.05$). Comparing G9 (30 J/cm²) and G7 (0 J/cm²), G9 showed significantly higher values for parameters Nv_{ost} , N_{ost} , Sv_t , and Sa_t ($P < 0.05$).

4 | DISCUSSION

Using design-based stereological methods, the present study estimated the trabecular surface area and the total number of osteocytes after low-level laser application, showing its positive effects when utilized in animals submitted to an experimental model of osteoporosis. It is known that LLLT uses low light irradiance, which is capable of influencing cell behavior through photophysical, photochemical, and photobiological effects in the irradiated tissue.¹⁷

This investigation showed that groups that received laser energy densities of 20 and 30 J/cm² presented higher stereological

TABLE 2 Means and SDs for osteocyte numerical density (N_{ost}), total osteocyte number (N_{ost}), trabecular surface density (S_v), and trabecular surface area (S_a) in groups with three sessions: G1 (0 J/cm²), G2 (20 J/cm²), and G3 (30 J/cm²)

	Groups			P
	G1	G2	G3	
$N_{v_{ost}} (\mu\text{m}^{-3})$	2964 ± 1186	9196 ± 6080	3384 ± 1540	0.049 (0-20 J/cm ²)
N_{ost}	$7.87 \times 10^{10} \pm 3.15 \times 10^{10}$	$4.34 \times 10^{11} \pm 2.87 \times 10^{11}$	$9.93 \times 10^{10} \pm 4.52 \times 10^{10}$	0.015 (0-20 J/cm ²) 0.021 (20-30 J/cm ²)
$S_v (\mu\text{m}^{-1})$	4.07 ± 0.51	10.58 ± 0.44	9.49 ± 2.73	0.000 (0-20 J/cm ²)
$S_a (\mu\text{m}^2)$	$10.79 \times 10^7 \pm 14.28 \times 10^6$	$49.43 \times 10^7 \pm 67.83 \times 10^6$	$25.46 \times 10^7 \pm 67.24 \times 10^6$	0.001 (0-20 J/cm ²)

TABLE 3 Means and SDs of osteocyte numerical density ($N_{v_{ost}}$), total osteocyte number (N_{ost}), trabecular surface density (S_v), and trabecular surface area (S_a) in groups with six sessions: G4 (0 J/cm²), G5 (20 J/cm²) and G6 (30 J/cm²)

	Groups			P
	G4	G5	G6	
$N_{v_{ost}} (\mu\text{m}^{-3})$	2719 ± 1547	3179 ± 405	4533 ± 27	0.022 (0-30 J/cm ²)
N_{ost}	$9.70 \times 10^{10} \pm 5.52 \times 10^{10}$	$1.70 \times 10^{11} \pm 2.16 \times 10^{10}$	$2.05 \times 10^{11} \pm 1.23 \times 10^9$	0.014 (0-20 J/cm ²) 0.000 (0-30 J/cm ²)
$S_v (\mu\text{m}^{-1})$	25.87 ± 6.32	53.31 ± 9.35	96.72 ± 27.07	0.041 (0-20 J/cm ²) 0.034 (0-30 J/cm ²)
$S_a (\mu\text{m}^2)$	$10.50 \times 10^8 \pm 33.82 \times 10^7$	$23.35 \times 10^8 \pm 41.41 \times 10^7$	$50.69 \times 10^8 \pm 14.57 \times 10^8$	0.043 (0-20 J/cm ²) 0.028 (0-30 J/cm ²)

TABLE 4 Means and SDs of osteocyte numerical density ($N_{v_{ost}}$), total osteocyte number (N_{ost}), trabecular surface density (S_v), and trabecular surface area (S_a) in groups with 12 sessions: G7 (0 J/cm²), G8 (20 J/cm²) and G9 (30 J/cm²)

	Groups			P
	G7	G8	G9	
$N_{v_{ost}} (\mu\text{m}^{-3})$	2527 ± 606	3676 ± 1449	5364 ± 1124	0.004 (0-30 J/cm ²)
N_{ost}	$1.25 \times 10^{11} \pm 3.00 \times 10^{10}$	$1.95 \times 10^{11} \pm 7.69 \times 10^{10}$	$3.51 \times 10^{11} \pm 7.36 \times 10^{10}$	0.000 (0-30 J/cm ²) 0.005 (20-30 J/cm ²)
$S_v (\mu\text{m}^{-1})$	32.37 ± 5.78	51.18 ± 6.30	125.58 ± 38.10	0.042 (0-30 J/cm ²)
$S_a (\mu\text{m}^2)$	$16.15 \times 10^8 \pm 31.24 \times 10^7$	$27.21 \times 10^8 \pm 35.34 \times 10^7$	$77.28 \times 10^8 \pm 19.40 \times 10^8$	0.047 (0-20 J/cm ²) 0.014 (0-30 J/cm ²)

parameters compared to those that received 0 J/cm². Among the groups that received three sessions of LLLT, a laser energy density of 20 J/cm² resulted in a higher total osteocyte number (N_{ost}) and an increased trabecular surface area (S_a). It has already been demonstrated that LLLT is capable of stimulating proliferation of human osteoblastic cell lines without modifying their morphological characteristics. LLLT was also able to increase specific protein secretion for bone cell differentiation, as well as calcium deposition and alkaline phosphatase activity. Thus, laser treatment increases cell proliferation and also influences osteogenic maturation.¹⁸ Mesenchymal stem cells derived from bone marrow irradiated with a low-level laser presented an increase in differentiation and proliferation.¹⁹ Our results are in agreement with the literature, suggesting that LLLT at an energy density of 20 J/cm² promoted positive effects on osteoblast proliferation and differentiation, increasing the total number of osteocytes.

When LLLT was applied over six sessions, a laser energy density of 30 J/cm² produced a larger increase in trabecular surface area compared to LLLT at 20 J/cm², and increases in osteocyte number and trabecular surface area compared to the control group. These results suggest that LLLT at an energy density of 30 J/cm² influenced osteoblastic proliferation and differentiation in the early period after the creation of the bone defect (7 days), reflected in an increased trabecular surface area after six sessions compared to controls. On the other hand, LLLT at an energy density of 30 J/cm² produced a better response after 13 days. Previous studies have reported that LLLT favors cell proliferation and differentiation,^{18,19} suggesting that after 13 days of bone repair, LLLT at an energy density of 30 J/cm² produced the same effect seen with 20 J/cm² after 7 days. It is possible that after 13 days, the treatment might have promoted an increase in the expression of the inflammatory mediator Cox-2

(cyclo-oxygenase-2). An increase in Cox-2 might contribute to an early recruitment of preosteoblasts and osteoblasts, leading to the presence of organized tissue and early deposition of neoformed bone.^{5,20} Supporting these results, laser treatment might promote the expression of the osteogenic markers Runx2, Bmp-9, and Rankl, since higher expression of Runx2 and Rankl has been found in diabetic rats after laser therapy.²¹ Thus, it is possible that rats subjected to an experimental model of osteoporosis may present higher expression of these markers, culminating in a greater osteoblastic differentiation, reflected in higher osteocyte numbers and increased trabecular surface area. These results are also in agreement with findings by Ré Poppi et al.²² Despite the fact that these authors used different wavelengths (660 and 880 nm) from those used in this study, they also observed higher densities of osteoblasts, fibroblasts, and immature osteocytes in the femur area of ovariectomized rats after 14 days compared to non-irradiated animals.

Another explanation for the increased number of osteocytes observed in this study might be that LLLT is able to regulate the Wnt pathway. Zhang et al.²³ showed that LLLT promotes the entry of β -catenin into the nucleus, and activates the osteogenic effect of the Wnt pathway to promote bone formation and inhibit bone resorption by osteoclasts.

In this study, the group that received laser treatment for 12 sessions at an energy density of 20 J/cm² showed only an increased trabecular surface area compared to the non-irradiated group. The samples from the animals receiving LLLT at an energy density of 30 J/cm² presented the highest stereological parameters, reflected in a higher total number of osteocytes and greater trabecular surface area, in agreement with the results of Ré Poppi et al.²²

The literature shows that estrogen plays an important role in the control of osteocyte apoptosis and its maintenance. Estrogen deficiency may compromise osteocyte viability, reducing bone capacity to respond adequately to applied forces,²⁴ since mechanical behavior might be affected by cell density.²⁵ Therefore, an energy density of 30 J/cm² applied for six and 12 sessions would promote an increase in osteocyte differentiation, which in turn would also promote better bone function, allowing a better response of this tissue when forces are applied.

The increase in the number of osteocytes following LLLT at an energy density of 30 J/cm² for six and 12 sessions might have produced an increase in secretion of sclerostin. Sclerostin is a protein intimately associated with the regulation of mineralization, callous ossification, and bone remodeling, suggesting it plays a critical role in bone consolidation after bone injury.²⁶

The results obtained in this study lead to the conclusion that LLLT stimulates bone neoformation, as shown by increased trabecular surface area and the total number of osteocytes, especially when utilizing a laser energy density of 30 J/cm² for six and 12 sessions. The data might influence application of this therapy and bring clinical benefits when treatment designed to improve bone neoformation is needed.

ACKNOWLEDGEMENTS

We thank FAPESP (São Paulo Research Foundation - Processes no. 2011/50686-0), CNPq (National Council for Scientific and

Technological Development) and National Institute and Technology - Translational Medicine (INCT.TM) for financial support.

CONFLICT OF INTEREST

None.

AUTHOR CONTRIBUTIONS

SS, SCHR, KFBP, and AAC conceived and designed the study. LGS, LMNG, and MP performed the animal surgeries. PHS, MAR, VR, and DLP performed the histological processing. PHS acquired the histological images and wrote the main manuscript. SS and SCHR performed and analyzed the data.

ORCID

Selma Siessere  <https://orcid.org/0000-0001-9756-3771>

REFERENCES

1. Tella SH, Gallagher JC. Prevention and treatment of postmenopausal osteoporosis. *J Steroid Biochem Mol Biol.* 2014;142:155-170.
2. Consensus development conference: prophylaxis and treatment of osteoporosis. *Am J Med.* 1991;90:107-110.
3. Hernlund E, Svedbom A, Ivergård M, et al. Osteoporosis in the European Union: medical management, epidemiology and economic burden. A report prepared in collaboration with the International Osteoporosis Foundation (IOF) and the European Federation of Pharmaceutical Industry Associations (EFPIA). *Arch Osteoporos.* 2013;8:136.
4. Kanis JA, McCloskey EV, Johansson H, et al. European guidance for the diagnosis and management of osteoporosis in postmenopausal women. *Osteoporos Int.* 2013;24:23-57.
5. Tim CR, Pinto KNZ, Rossi BRO, et al. Low-level laser therapy enhances the expression of osteogenic factors during bone repair in rats. *Lasers Med Sci.* 2014;29:147-156.
6. de Vasconcellos LM, Barbara MA, Deco CP, et al. Healing of normal and osteopenic bone with titanium implant and low-level laser therapy (GaAIA): a histomorphometric study in rats. *Lasers Med Sci.* 2014;29:575-580.
7. Sella VR, do Bomfim FR, Machado PC, da Silva Morsoleto MJ, Chohfi M, Plapler H. Effect of low-level laser therapy on bone repair: a randomized controlled experimental study. *Lasers Med Sci.* 2015;30:1061-1068.
8. Marques L, Holgado LA, Francischone LA, Ximenez JP, Okamoto R, Kinoshita A. New LLLT protocol to speed up the bone healing process-histometric and immunohistochemical analysis in rat calvarial bone defect. *Lasers Med Sci.* 2015;30:1225-1230.
9. Scalize PH, de Sousa LG, Regalo SC, et al. Low-level laser therapy improves bone formation: stereology findings for osteoporosis in rat model. *Lasers Med Sci.* 2015;30:1599-1607.
10. Oliveira LSS, Araújo AA, Araújo Júnior RF, Barboza CAG, Borges BCD, Silva JSP. Low-level laser therapy (780 nm) combined with collagen sponge scaffold promotes repair of rat cranial critical-size defects and increases TGF- β , FGF-2, OPG/RANK and osteocalcin expression. *Int J Exp Pathol.* 2017;98:75-85.
11. Kalu DN. The ovariectomized rat model of postmenopausal bone loss. *Bone Miner.* 1991;15:175-191.
12. Marcondes FK, Bianchi FJ, Tanno AP. Determination of the estrous cycle phases of rats: some helpful considerations. *Braz J Biol.* 2002;62:609-614.

13. Chicarelli M, Ramos FMM, Manzi FR, Novaes PD, Bóscolo FN, Almeida SM. Effect of gamma rays on the bone repair process in rats with estrogen deficiency. *Braz Oral Res.* 2007;21:75-80.
14. Nyengaard JR, Gundersen HJG. The isector: a simple and direct method for generating isotropic, uniform random sections from small specimens. *J Microsc.* 1992;165:427-431.
15. Gundersen HJ. The smooth fractionator. *J Microsc.* 2002;207:191-210.
16. Gundersen HJ, Bagger P, Bendtsen TF, et al. The new stereological tools: disector, fractionator, nucleator and point sampled intercepts and their use in pathological research and diagnosis. *APMIS.* 1998;96:857-881.
17. Karu T. Photobiology of low-power laser effects. *Health Phys.* 1989;56:691-704.
18. Bloise N, Ceccarelli G, Minzioni P, et al. Investigation of low-level laser therapy potentiality on proliferation and differentiation of human osteoblast-like cells in the absence/presence of osteogenic factors. *J Biomed Opt.* 2013;18:128006.
19. Soleimani M, Abbasnia E, Fathi M, Sahraei H, Fathi Y, Kaka G. The effects of low-level laser irradiation on differentiation and proliferation of human bone marrow mesenchymal stem cells into neurons and osteoblasts – an in vitro study. *Lasers Med Sci.* 2012;27:423-430.
20. Matsumoto MA, Ferino RV, Monteleone GF, Ribeiro DA. Low-level laser therapy modulates cyclo-oxygenase-2 expression during bone repair in rats. *Lasers Med Sci.* 2009;24:195-201.
21. Patrocínio-Silva TL, de Souza AM, Goulart RL, et al. The effects of low-level laser irradiation on bone tissue in diabetic rats. *Lasers Med Sci.* 2014;29:1357-1364.
22. Ré Poppi R, Da Silva AL, Nacer RS, et al. Evaluation of the osteogenic effect of low-level laser therapy (808 nm and 660 nm) on bone defects induced in the femurs of female rats submitted to ovariectomy. *Lasers Med Sci.* 2011;26:515-522.
23. Zhang RF, Wang Q, Zhang AA, et al. Low-level laser irradiation promotes the differentiation of bone marrow stromal cells into osteoblasts through the APN/Wnt/ β -catenin pathway. *Eur Rev Med Pharmacol Sci.* 2018;22:2860-2868.
24. Tomkinson A, Gevers EF, Wit JM, Reeve J, Noble BS. The role of estrogen in the control of rat osteocyte apoptosis. *J Bone Miner Res.* 1998;13:1243-1250.
25. Hemmatian H, Bakker AD, Klein-Nulend J, van Lenthe GH. Aging, osteocytes, and mechanotransduction. *Curr Osteoporos Rep.* 2017;15:401-411.
26. Compton JT, Lee FY. A review of osteocyte function and the emerging importance of sclerostin. *J Bone Joint Surg Am.* 2014;96:1659-1668.

How to cite this article: Scalize PH, de Sousa LG, Gonçalves LMN, et al. Low-level laser therapy enhances the number of osteocytes in calvaria bone defects of ovariectomized rats. *Animal Model Exp Med.* 2019;2:51–57.
<https://doi.org/10.1002/ame2.12056>